

Mesosphere Sodium Column Density and the Sodium Laser Guide Star Brightness

Jian Ge^a, J.R.P. Angel^a, B.D. Jacobsen^a, T. Roberts^a, T. Martinez^a, W. Livingston^b,
B. McLeod^c, M. Lloyd-Hart^a, P. McGuire^a, R. Noyes^c

^aSteward Observatory, The University of Arizona, Tucson, AZ 85721, USA

^bNational Solar Observatory, Tucson, AZ 85726, USA

^cCenter for Astrophysics, MS 20, 60 Garden Street, Cambridge, MA 02138, USA

ABSTRACT

The first time simultaneous measurements of sodium column density and the absolute flux from a sodium laser guide star, created by a monochromatic 3 W cw laser, tuned to the peak of the sodium D₂ hyperfine structure, were conducted at the MMT and CFA 60 inch telescope in 1997. The results show that linearly and circularly polarized laser returns are proportional to the simultaneous sodium column density. Moreover, circularly polarized laser provides $\sim 30\%$ increase in fluorescent return over linearly polarized laser. A laser guide star with $R = 10.3$ mag. or absolute flux of 8.4×10^5 photons $s^{-1} m^{-2}$, could be formed from a 1 watt projected circularly polarized sodium laser beam when sodium layer abundance $N(\text{Na}) = 3.7 \times 10^9$ cm^{-2} . Together with the distributed column density measurements (e.g. seasonal and diurnal variations), we can project laser power requirements for any specified guide star brightness.

The mesosphere sodium column density variation was measured above Tucson sky throughout the year, through sodium absorption line measurements in stellar and solar spectra. Previous measurements, e.g. Papen et al, 1996, have not been made at this latitude (32 degrees). Further, our absorption method is more direct and may be more accurate than the lidar methods normally used. The seasonal variation amplitude is smaller than that at higher latitudes. While the annual mean sodium column density tends to be lower than at higher latitudes. Diurnal sodium column density tends to vary by as much as a factor of two within an hour.

1. INTRODUCTION

Adaptive optics systems for atmospheric-turbulence compensation require a bright point reference source of light for measuring and correcting wave-front distortions. The bright source must be within a small field of view of the astronomical sources of interest. While some sources are bright enough to provide the required information themselves, most astronomical sources of interest are too faint. For this reason, general astronomical use of adaptive optics requires a laser beacon to provide the wavefront information. An artificial laser beacon can be created by backscattered light from a ground-based laser beam pointed at the scientific source. For example, an artificial guide star is created by focusing a sodium laser beam tuned to the sodium D₂ line at 589 nm wavelength on the mesosphere sodium layer at about 90 km altitude. Several groups in the world have begun to explore the use of sodium laser guide star technique for astronomical adaptive optics (e.g. Jacobsen et al. 1993; Max et al. 1994; Jelonek et al. 1994; Avicola et al. 1994). In the Fall 1996, our group has successfully closed the laser guide star adaptive optics tip-tilt system loop and make improvements in the image quality (Lloyd-Hart et al. 1997). In the early 1997, Livermore laser guide star group has also successfully closed their high order AO loop and make significant image corrections (Olivier et al. 1997). These experiments demonstrate the possibility of sodium laser guide star technique in adaptive optics applications. However, for the sodium laser guide star adaptive optics technique, there is as yet no consensus on the optimum laser and power. The choice depends not only on the laser power, but on the inherently different pulse formats and frequency purity of different laser types. Theoretical calculations predict differences in return for the same power and column density up to a factor 5 (Milonni & Telle, 1996, private communication), according to pulse format, but these have yet to be confirmed experimentally. Thus, experiments that measure column density

Other author information: (Send correspondence to Jian Ge)

J. G.: Email: jge@as.arizona.edu; WWW: <http://qso.as.arizona.edu/~jge>; Telephone: 520-621-6535; Fax: 520-621-1532

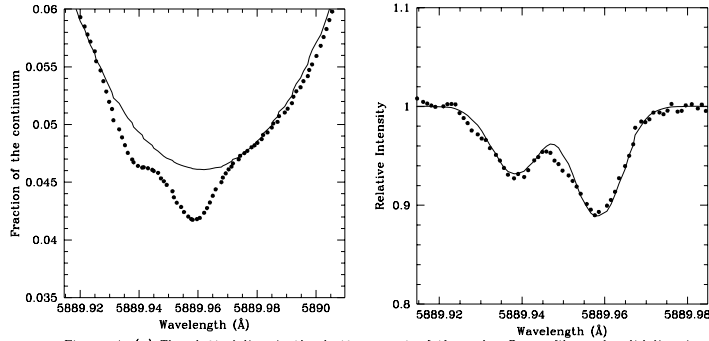


Figure 1. (a) The dotted line is the bottom part of the solar D_2 profile and solid line is the computer generated least square fit. (b) The residual spectrum after the solar D_2 profile being extracted. The dotted line is the Telluric D_2 hyperfine profile and the solid line is the best fit.

and details of the excitation and scattering properties of sodium atoms in the sodium layer are very important to refine the design parameters of the laser and assess the power requirement.

Simultaneous local observations of the sodium column density and the laser return are necessary to obtain the fundamental relationship between the magnitude of the laser guide star and sodium abundance. Previous studies have shown that the column density of the sodium layer varies with time, including long term seasonal variations and short term variations (e.g. Papen 1996), and also varies with latitude (Hunten 1966; Magie et al. 1978; Papen et al. 1996). A simultaneous measurement of column density and guide star brightness has not been done before. This together with the measurements of sodium layer abundance variation will provide a reference for the design of our future sodium laser for the MMT 6.5 m AO system as well as other sodium laser guide star systems in the world.

In this paper we will briefly report on seasonal sodium layer column density variations over Tucson (Ge, Angel, & Livingston 1997, in preparation), simultaneous sodium laser return and mesosphere sodium abundance measurements. We will compare the new results with previous results by other groups and finally draw some initial conclusions.

2. OBSERVATIONS AND REDUCTIONS

2.1. Seasonal Mesosphere Sodium Observations and Reductions

The observations of the seasonal mesosphere sodium variation over Tucson were conducted with the National Solar Observatory McMath solar telescope on Kitt Peak. The high resolution 13.5 m main spectrometer with the 632 g/mm grating and predisperser was used to provide resolution of about 2.6×10^6 (theoretical value). The receiver is a photomultiplier with no readout noise, no bias and no cosmic ray. Solar sodium D_2 absorption spectra are one-dimensional and were obtained in 1 minute integration.

The main method for the data reduction is to fit the generated Voigt profile to the bottom of the solar D_2 line. The main object of the computer program was to compute a set of optimum parameters that could generate the best least-square fit of the model to the data (excluding the mesosphere D_2 absorption region). We then extracted the solar absorption by removing the fitted profile to obtain the residual spectrum which contains the tiny absorption lines from the sodium layer. The typical solar spectrum near the bottom of the D_2 sodium line and residual telluric D_2 absorption spectra are shown in Figure 1.

2.2. Simultaneous Sodium Laser Return and Column Density Measurements

The simultaneous measurements of mesosphere sodium abundance and laser return were made in the nights of March 23rd and May 20th, 1997. Both nights were photometric. The sodium return experiments were conducted at the MMT on Mt. Hopkins. The telescope was pointed to the direction of standard stars, which were close to the stars for observing telluric sodium absorption. At the same time, telluric sodium absorption spectra were recorded by the Advanced Fiber Optic Echelle spectrograph (AFOE) at the CFA 60" telescope about 1 km away from the MMT on the same mountain. Therefore, similar sodium layer patches were observed by both telescopes.

The laser we applied is a continuous-wave dye laser pumped by 30 watts argon ion laser. A traveling-wave ring cavity design for the dye laser was used to provide a single longitudinal mode at high powers. Tuning of the ring-cavity laser was made by adding several frequency selective elements such as a three-plate birefringent filter and

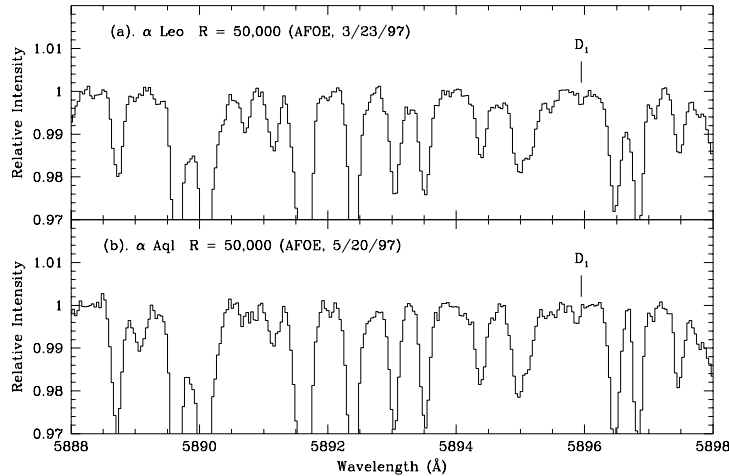


Figure 2. Typical Telluric sodium D_1 absorption spectra obtained at the CFA 60 inch.

two etalons to the cavity. The detailed design and performance are described by Roberts et al. (1997). The laser system produced a stable sodium laser output power of about 2.4 Watts, tuned to the peak of D_2 hyperfine structure during the return experiments. The full width at half maximum (FWHM) of the laser line profile is less than 10 MHz. However, vibrations in the laser system, especially in the dye jet, could produce frequency jitter of about 0.7 GHz (peak-to-valley). A polarization compensator made of MgF_2 crystal has been introduced in the sodium laser beam to change the laser polarization during the observations. After the sodium laser passed through the whole laser beam projector system (Jacobsen & Angel 1997), power projected to the sodium layer was typically 0.9W. There are 14 transmissive and 7 reflective surfaces between the Dye laser output and the laser beam projector output, which provides about total 45% transmission. The R filter used for the photometric measurements transmits 79% photons at the D_2 wavelength. Therefore, the total throughput of the laser projection is about 36%, which is consistent with the sodium laser power measurement results. The laser star and standard star images were recorded by a thermally cooled Axiom CCD camera mounted on the telescope. The data were reduced in the standard way with the IRAF package. The photometry of laser guide stars was measured by using the IRAF package PHOT. The estimated error of the photometry is 2.5% based on the standard star flux measurements.

The spectrograph we used for measuring the telluric sodium abundance provides spectral resolution of $R \sim 50,000$, which cannot provide enough resolution to separate D_2 line from nearby water vapor lines. We therefore use D_1 , which has half the D_2 line strength, instead. The equivalent width of typical telluric sodium D_1 absorption line is less than 1 mÅ. In order to measure the sodium abundance better than 15% error, signal to noise ratio (S/N) of at least 1,000 is required. With 16 bits CCD readout electronics, S/N of ~ 500 can be reached in each frame. On the other hand, once S/N reaches about 500, CCD pixel-to-pixel variation will limit S/N go any higher. To solve this problem, we took ~ 100 frames of flat and combined them, and divided the combined object frames (α Leo in the March run, and α Aql in the May run) by the combined flat. The final S/N of combined object frame can reach as high as $\sim 2,000$, which is good enough for the accurate sodium abundance measurements. Fig. 2(a),(b) show typical telluric D_1 spectra from both observation runs.

3. RESULTS

3.1. Seasonal Sodium Abundance Results

Because the mesosphere sodium absorption is normally very weak, e.g. the typical optical depth at the center of the absorption line is $\tau_0 \sim 0.04 \ll 1$, it is appropriate to assume that the absorption line is in the linear portion of the curve of growth, where the column density of the atoms is proportional to the equivalent width. The number of sodium atoms per square centimeter in the line of sight is then given by

$$N = \frac{mc^2}{\pi e^2 f} \int_0^\infty \frac{I_0(\nu) - I(\nu)}{I_0(\nu)} d\nu = 1.130 \times 10^{20} \frac{W_\lambda}{f\lambda^2} \text{ cm}^{-2}, \quad (1)$$

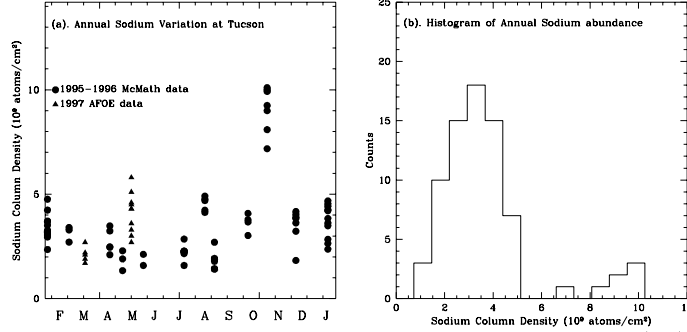


Figure 3. Annual mesosphere sodium column density distribution above Kitt Peak (32°N). Annual mean is $3.7 \times 10^9 \text{ cm}^{-2}$.

where W_λ is the equivalent width, and both W_λ and λ are in unit of Å, f is the oscillator strength ($f = 0.3944, 0.2367$ for the 5889.9584 Å , 5889.9386 Å hyperfine lines of the D_2 , respectively; Morton 1991). The error resulted from neglecting saturation effect was estimated to be less than about 2.5%, which is within the measurement error of about 5% for the whole seasonal observation results.

Figure 3 shows the seasonal variations of the sodium layer column density above Tucson between February 1995 and January 1996. Since we observed the Sun at different airmass, we need to normalize the measured column densities to the values at the zenith. The relationship between the airmass and the sodium layer thickness can be expressed as

$$\sec\phi = \frac{1}{\sqrt{1 - \left(\frac{r_e}{r_e + H}\right)^2 \left(1 - \frac{1}{\sec^2 z}\right)}} \quad (2)$$

where $\sec\phi$ is the thickness factor of the sodium layer, $r_e = 6378.5 \text{ km}$ is the radius of the Earth, the height of the sodium layer above Kitt Peak, $H = 90 \text{ km}$ is assumed, and $\sec z$ is the airmass. Thus, the value of $\sec\phi$ is 1.0 when $\sec z = 1.0$ and it is about 6.0 when $\sec z \rightarrow \infty$. The column densities in Figure 3 represent the values at the zenith. Each point represents an averaged value within 4-8 minute integration time. The dominant error in these measurements is from the solar D_2 profile fitting, which is estimated to be about 5%. The scattering in the measured values during each day therefore represents the real short term variation. The variation amplitude could be as large as a factor of two within a short period of time (on the order of hours), which has also been found at other latitude by Lidar technique (e.g. Papen et al. 1996). There is also a strong trend of seasonal variation in this figure. Higher sodium abundance was reached during the winter time with an average of $\sim 4 \times 10^9 \text{ cm}^{-2}$, except October data points, when the sodium abundance is extreme large compared with the values in the neighbour months. This extreme high abundance could be caused by sporadic events during that day, caused by such as meteor events or geomagnetic activity (Papen et al. 1996). Generally, lower sodium abundance was reached during the summer time with an average value of $\sim 2 \times 10^9 \text{ cm}^{-2}$. The annual mean is $3.7 \times 10^9 \text{ cm}^{-2}$ is lower than that at higher latitude (Papen et al. 1996). If we neglect the data points from the October run, the variation amplitude within a year period from Tucson (32° N) is smaller than that at higher latitudes (e.g. Urbana, 40° N . Papen et al. 1996; Haute-Provence, 44° N . Magie et al. 1978). These new measurements from different latitudes confirm the latitude-related trend shown in earlier studies using twilight emission line technique (Hunten 1966). Detailed analysis on the seasonal, daily, nightly and hourly variation of sodium abundance above Kitt Peak can be seen in our future paper (Ge, Angel & Livingston 1997).

3.2. Simultaneous Sodium Return and Abundance Results

Table 1 and 2 show the measurements of simultaneous absolute return flux from linearly and circularly polarized sodium laser beams and sodium column density from the March and May runs, 1997, which also include corresponding R magnitude. Fig. 4(a)(b) show the relationship between the absolute laser guide star flux and sodium abundance at the zenith. Both backscatters from circular and linear polarization are proportional to sodium column density. The absolute return flux range is consistent with that from our previous return measurements though no simultaneous sodium abundance being measured at that time (Jacobsen et al. 1993). Further, the circular polarization provides $\sim 30\%$ increase in fluorescent return over linear polarization. Based on these results, a laser guide star with $R = 10.3 \text{ mag.}$ or absolute flux of $8.4 \times 10^5 \text{ photons s}^{-1} \text{ m}^{-2}$, could be formed from a 1 watt projected circularly polarized

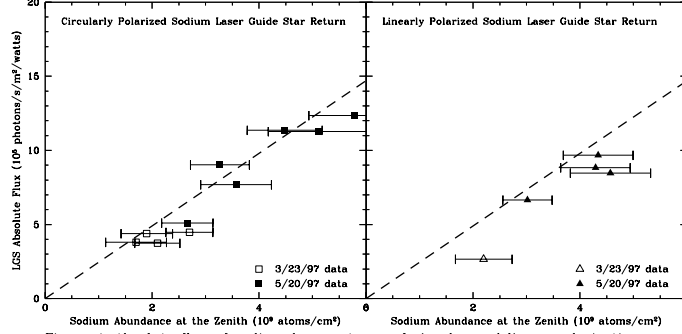


Figure 4. Absolute flux of sodium laser returns of circular and linear polarization vs. sodium abundance at Zenith

sodium cw laser beam when sodium layer abundance $N(\text{Na}) = 3.7 \times 10^9 \text{ cm}^{-2}$, which is the mean value of annual sodium abundance in the sodium layer at the latitude of 32° N (Tucson).

Table 1. Simultaneously Linearly Polarized Laser Return and Column Density Measurements

No.	Time (MT)	Absolute Return Flux at Zenith ($10^5 \text{ Photons/m}^2/\text{s/W}$)	Sodium Column Density at Zenith (10^9 atoms/cm^2)	R magnitude/W
1	1h13m, 3/23/97	2.6	2.2 ± 0.5	11.5
2	3h18m, 5/20/97	6.6	3.0 ± 0.5	10.5
3	3h23m, 5/20/97	9.6	4.3 ± 0.7	10.1
4	3h33m, 5/20/97	8.5	4.6 ± 0.7	10.3
5	3h39m, 5/20/97	8.8	4.3 ± 0.7	10.2

Table 2. Simultaneously Circularly Polarized Laser Return and Column Density Measurements

No.	Time (MT)	Absolute Return Flux at Zenith ($10^5 \text{ Photons/m}^2/\text{s/W}$)	Sodium Column Density at Zenith (10^9 atoms/cm^2)	R magnitude/W
1	12h32m, 3/23/97	3.8	1.7 ± 0.5	11.1
2	1h16m, 3/23/97	3.7	2.1 ± 0.4	11.2
3	1h26m, 3/23/97	4.4	1.9 ± 0.5	11.0
4	1h55m, 3/23/97	4.5	2.7 ± 0.4	11.0
5	2h45m, 5/20/97	11.3	4.5 ± 0.7	10.0
6	3h08m, 5/20/97	9.0	3.3 ± 0.6	10.2
7	4h04m, 5/20/97	7.7	3.6 ± 0.7	10.4
8	4h08m, 5/20/97	5.1	2.7 ± 0.5	10.8
9	4h14m, 5/20/97	11.3	5.1 ± 0.9	10.0
10	4h18m, 5/20/97	12.3	5.8 ± 0.9	9.9

The backscatter enhancement by circular polarization is consistent with the theoretical prediction (Morris 1994; Milonni, Fugate & Telle 1997), and also qualitatively consistent with the LGS measurement report by Jelonek et al. (1994). The dashed lines in Fig. 4(a)(b) are the theoretical curves generated from the following simple theoretical estimate

$$N_r = N_t \epsilon \frac{A_c}{4\pi H^2} T^2 1.5, \quad (3)$$

where N_r is backscatter in unit of photons s^{-1} , $N_t = 3.0 \times 10^{18}$ photons s^{-1} is the total output flux of 1 watt power, A_c is the photon collector area, $H = 90$ km, atmosphere transmission $T \approx 0.8$ during the experiments. $\epsilon = \sigma_P N_{Na}$, where N_{Na} is the sodium column density, and peak cross section of D_2 hyperfine $\sigma_P = 8.8 \times 10^{-12}$ cm^2 is applied because the line width of < 10 MHz for the cw dye laser tuned to the hyperfine peak is very narrow compared to 1.19 GHz for the FWHM of D_2 hyperfine line (Happer et al. 1994). The angular dependent scattering factor, 1.5, for the backward is also used in equation (3) (Jeys 1991). The simple theoretical prediction matches the circular polarization measurements very well. However, the results from preliminary theoretical studies including the Earth's magnetic field and optical pumping effects predicted a factor of two higher return than that we have measured (Milonni 1997, private communication). The difference could be caused by the premature theoretical studies or possible less measured return flux caused by the sodium laser frequency instability during the return experiments. If the laser frequency instability is confirmed in the future MMT sodium guide star experiments, then we should consider this frequency instability effect in our measured results.

4. DISCUSSION

Annual mesosphere sodium abundance measurements show that there is long term seasonal variation at the latitude of 32° N., and variation amplitude is about a factor of two. Sodium column density could also vary by a factor of two with a short period of time (hourly). Therefore the laser power dynamical range should be at least designed to match the sodium abundance variation range of a factor of two in order to provide enough return photons for LGS AO system to get enough image correcting power. The preliminary results from the simultaneous measurements of the sodium laser return and sodium layer abundance suggest that a circularly polarized sodium cw dye single longitudinal mode laser with 3 watts projected power on sky tuned to the peak of D_2 hyperfine will meet the LGS brightness requirement of 9.5 mag. for the future MMT 6.5 m telescope LGS AO system (Sandler et al. 1994), even when sodium abundance reaches the lowest point in the seasonal variation curve (Fig. 3).

ACKNOWLEDGEMENTS

We thank MMT staffs for great patience and help during our FASTRAC II run. We thank Perry Berling and Jim Peters for helping collecting and reducing 60 inch AFOE raw data. We thank L. Wallace for helpful discussions. We thank D. Lytle for his helpful program to convert the raw solar date format to standard IRAF format. This work has been supported by the Air Force Office of Scientific Research under grant number F49620-94-1-00437 and F 49620-96-1-0366.

REFERENCES

- Avicola, K. et al. 1994, JOSA, 11, 825
Happer, W., MacDonald, G.J., Max, C.E., & Dyson, F.J. 1994, JOSA, 11, 263
Hunten, D.M. 1967, Space Science Reviews, 6, 493
Jacobsen, B. et al. 1993, SPIE, 2201, 342
Jacobsen, B. & Angel, R., 1997, this proceeding
Jelonek, M.P. et al. 1994, JOSA, 11, 806
Jeys, T.H. 1991, The Lincoln Lab. Journal, 4, 133
Lloyd-Hart, M. et al. 1997, ApJ Letter, submitted
Max, C.E. et al. 1994, JOSA, 11, 813
Magie, G. et al. 1978, Planet. Space Sci. 26, 27
Milonni, P.W., Fugate, R. Q., & Telle, J.M. 1997, in preparation
Morris, J.R. 1994, JOSA, 11, 832
Morton, D.C. 1991, ApJS, 77, 119
Olivier, S.S. et al. 1997, SPIE, 3126, in press
Roberts, T., et al. 1997, this proceeding
Papen, G.C., Gardner, C.S. & Yu, J. 1996, in Adaptive Optics, Vol. 13, OSA Technical Digest Series (Optical Society of America, Washington DC), 96
Sandler, D.G., et al. 1994, JOSA, 11, 925